Advances in Geo-Energy Research

Vol. 10, No. 3, p. 159-173, 2023

Original article

Feasibility analysis of storing solar energy in heterogeneous deep aquifer by hot water circulation: Insights from coupled hydro-thermo modeling

Yanyong Wang[1,2,3], Kunpeng Zhong[1], Yihua Gao[5], Zhenjie Sun[1], Rencheng Dong[4], Xiaoguang Wang[1,2,3]*

[1]*College of Energy, Chengdu University of Technology, Chengdu 610059, P. R. China*

[2]*National Key Laboratory of Oil and Gas Reservoir Geology and Exploitation, Chengdu University of Technology, Chengdu 610059, P. R. China*

[3]*Tianfu Yongxing Laboratory, Chengdu 610213, P. R. China*

[4]*Oden Institute for Computational Engineering and Sciences, The University of Texas at Austin, Austin 78712, USA*

[5]*CNOOC Research Institute Co., Ltd., Beijing 100028, P. R. China*

Keywords:
Thermal energy storage
solar energy
geothermal
deep aquifer
hydro-thermo coupling

Cited as:
Wang, Y., Zhong, K., Gao, Y., Sun, Z., Dong, R., Wang, X. Feasibility analysis of storing solar energy in heterogeneous deep aquifer by hot water circulation: Insights from coupled hydro-thermo modeling. Advances in Geo-Energy Research, 2023, 10(3): 159-173.
https://doi.org/10.46690/ager.2023.12.03

Abstract:
Storing solar energy in the subsurface as heat is a promising way for energy storage and conversion, which has a great potential to address the temporal and spatial mismatch between energy demand and supply. Thermal energy storage in deep aquifers can convert intermittent solar energy into stable high temperature geothermal energy. In this study, a new solar energy storage and conversion system is proposed where solar energy is firstly converted into heat using parabolic troughs and then stored in deep aquifers by high temperature hot water circulation. The geostatistical modelling and hydro-thermo coupling simulations are adopted to investigate the feasibility and efficiency of solar energy storage in deep aquifers. Specifically, how rock permeability heterogeneity (in terms of autocorrelation length and global permeability heterogeneity) impacts the temporal and spatial evolution of temperature distribution and storage efficiency is examined. The simulation results indicate that increased horizontal autocorrelation length and global heterogeneity may accelerate thermal breakthrough, deteriorating storage efficiency. High permeability heterogeneity may also lead to high injection pressure. Deep aquifers with small horizontal autocorrelation lengths and low global heterogeneity tend to have higher storage efficiency. These findings may improve our understanding of solar energy storage mechanism in deep aquifers and guide field applications.

1. Introduction

To achieve carbon neutrality, a low carbon energy system must be built to substantially reduce greenhouse gas emissions (Song et al., 2023). Over the next few decades, the energy system will continuously transition from conventional fossil fuels to clean, renewable sources (Zhao and You, 2020; Liu and Taleghani, 2023). Renewable energy is currently the world's fastest growing energy source with tremendous growth expected to continue. However, renewable energy sources such as solar and wind power exhibit significant fluctuations and intermittency. The transition from fossil fuels to those with high renewable energy systems may create supply-demand imbalance. Short-term and seasonal energy storage is considered as an important and cost-effective way to balance variable renewable supply and integrate electricity and heat sectors in near 100% renewable systems (Gao et al., 2009; Wesselink et al., 2018; Fleuchaus et al, 2020a; Birdsell et al., 2021). In this context, energy storage is a prerequisite to bridge the gap

Yandy Scientific Press

*Corresponding author.
E-mail address: wangyanyong@cdut.edu.cn (Y. Wang); kunpengzhong11@gmail.com (K. Zhong); gyhupc@163.com (Y. Gao); sunzhenjie92@163.com (Z. Sun); rencheng_dong@utexas.edu (R. Dong); wangxiaoguang@cdut.edu.cn (X. Wang).

Received September 25, 2023; revised October 18, 2023; accepted November 7, 2023; available online November 11, 2023.

between the supply and demand of renewable energy.

Geothermal energy is a clean energy source that harnesses renewable heat from the Earth's core. Unlike solar and wind, geothermal energy is not affected by day-night cycles, weather, or seasons, allowing for 24/7 baseload power generation. The production performance of geothermal energy from different types of geothermal reservoirs has been thoroughly investigated in the past years (Xu et al., 2018; Ijeje et al., 2019; Shi et al., 2019; Yang et al., 2023), and geothermal energy extraction from porous aquifer is technically feasible (Zhang et al., 2016; Wang et al., 2018; Cui et al., 2022). Therefore, aquifer thermal energy storage has emerged as an effective way to store and convert solar energy (Kastner et al., 2017). Aquifer thermal energy storage can effectively convert intermittent renewables like solar energy into stable and dispatchable geothermal power.

Aquifer thermal energy storage is a proven technology that has been implemented for decades. Aquifer thermal energy storage can provide direct cooling in summer and low-temperature winter heating for heat pump evaporators. Aquifer thermal energy storage systems operate in the range of 2-30 °C. In past decades, aquifer thermal energy storage has been studied via numerical simulations and field applications (Sommer et al., 2013; Zhou et al., 2015; Major et al., 2018; Fleuchaus et al., 2020b). Compared to shallow aquifers, deep aquifers offer much greater heat storage capacity. Although shallow aquifer thermal energy storage is well understood, much less work has been done on heat storage in deep sedimentary reservoirs, which limits its large-scale deployment. The focus of this study is heat storage in deep confined aquifers with minimal regional groundwater flow. In such systems, heat loss is significantly reduced due to existing overburdens and formation temperature is higher due to natural geothermal gradient. Geothermal energy storage has emerged as a large-scale renewable energy storage method suited in high porosity, high permeability, water-saturated sedimentary basins (Green et al., 2021). However, horizontal and vertical permeability anisotropies in layered sedimentary rocks may lead to asymmetric temperature and pressure profiles away from a production/injection well, which needs to be considered when planning the optimal spacing between production and injection wells (Panja et al., 2021a). Numerical simulations indicate formation heterogeneity has insignificant impact on huff-puff type thermal storage system (Panja et al., 2021b). Winterleitner et al. (2018) found that meter-scale heterogeneities and density-driven flow significantly influence the performance of high temperature aquifer thermal energy storage. Jello et al. (2022) experimentally and numerically investigated converting oil and gas wells into advanced geothermal energy storages. They found a monthly alternating injection and production process can sustain a thermal storage efficiency of 82% (Jello et al., 2022). Shi et al. (2023) stimulated heat storage in deep aquifers, and found that lower porosity, conductivity and heat capacity in aquitards improve heat retention. Huang et al. (2021) investigate high temperature aquifer thermal energy storage in naturally fractured reservoirs and demonstrate that the presence of the discrete fracture networks increases thermal loss and reduce thermal recovery

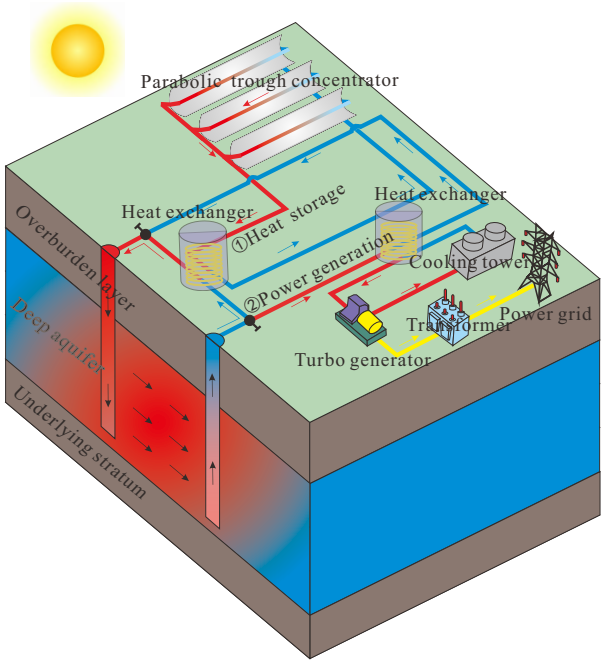

Fig. 1. Schematic for the proposed system of solar energy conversion and storage in deep aquifer.

efficiency compared to unfractured formations. Nevertheless, the higher injectivity in naturally fractured reservoirs makes them potential candidates for high temperature aquifer thermal energy storage (Huang et al., 2021). Ricks et al. (2022) analyzed the potential for geothermal plants to take advantage of the natural properties of confined, engineered geothermal reservoirs to store energy in the form of accumulated, pressurized geofluid and to provide flexible load-following generation. They found that such reservoirs can provide large and effectively free energy storage capacity and round-trip efficiencies comparable to grid-scale energy storage technologies.

In this study, the performance of a novel solar energy conversion and storage system is studied, which comprises a parabolic trough concentrator and a doublet well system (Fig. 1). The parabolic trough concentrates sunlight onto a focal line of concave mirrors through which working fluid (e.g., water), absorbing solar thermal energy. The heated water is then injected into a deep aquifer via an injection well, creating an artificial geothermal reservoir, while cold water is simultaneously extracted from the production well to maintain formation pressure. The produced water is treated at the surface then recycled through parabolic trough for reheating. With continued hot water circulation over time, intermittent solar input is converted into heat and stored in the subsurface. The heat storage performance of the system depends on various geological and engineering factors. The focus is on the impacts of spatial heterogeneity and buoyancy-driven hot water flow. A coupled hydro-thermo model is developed to simulate the transient flow and heat transfer behaviors within a confined porous aquifer. Sequential Gaussian simulation is applied to construct synthetic typical heterogeneous aquifer models. A series of numerical simulations are conducted to investigate solar energy storage process in deep aquifers by hot water

circulation. Improved understanding heat storage mechanisms of solar energy in heterogeneous aquifers can guide field-scale implementation and engineering design and deployment of large-scale, cost-effective aquifer thermal energy storage.

2. Theory and approach

2.1 Generation of three-dimensional heterogeneous aquifer

In this work, a three-dimensional (3D) model of confined porous aquifer, with the model dimension of 200 m in length, 200 m in width and 100 m in thickness, is applied to assess the feasibility of solar energy storage in the subsurface by hot water circulation and reveal the influences of different factors (e.g., buoyant flow, spatial heterogeneity) on thermal energy storage performance. For heterogeneous porous aquifers, the permeabilities of formation rock are assumed to follow a log-normal distribution, and thus can be reconstructed by using a sequential Gaussian simulation method (Deutsch and Journel, 1997). The spatial variability of permeabilities is correlated by adopting a spherical variogram, while the nugget effect is not considered during geological modeling. The porosities of the formation rock are then calculated based on the synthetic permeabilities by using an empirical correlation (Holtz, 2002), which can well predict the relationship between porosity and permeability for porous rock, as given by:

$$\phi = \left(\frac{k}{7\times 10^7}\right)^{1/9.61} \tag{1}$$

where k denotes the intrinsic permeability of formation rock, mD; ϕ stands for the effective porosity, fraction.

The dimensionless autocorrelation length (λ_D) and Dykstra-Parsons coefficient of permeability variation (V_{DP}) are adopted to describe the spatial heterogeneity of permeability fields quantitatively. λ_{Dh} or λ_{Dz} is defined as the ratio of horizontal or vertical autocorrelation length (λ_h or λ_z) to the model dimension along horizontal or vertical direction. V_{DP} is a dimensionless number to measure global permeability heterogeneity. V_{DP} ranges from 0 to 1. A uniform aquifer has a V_{DP} close to 0, whereas a severely heterogeneous aquifer has a V_{DP} close to 1. The detailed definitions and influencing factors of these two metrics can be referred to Wang et al. (2022).

2.2 Governing equations

In this study, the storage of solar energy in porous aquifer is considered as a thermo-hydro coupling process, with the effects of in-situ stress and rock fluids interactions being neglected. The governing equation for the mass conservation in terms of pore pressure can be described as:

$$\frac{\partial \phi \rho_w}{\partial t} + \nabla\cdot(\rho_w u_w) = q_w \tag{2}$$

where ρ_w denotes the density of water, kg/m^3; t is time, s; u_w is the seepage velocity of water in pore space, m/s; q_w is the source term, kg/(m^3·s).

In thermal energy storage process, the pore space within aquifer is assumed to be fully saturated with formation water, and the phase change of water is ignored under the operation pressure and temperature conditions. In such condition, single-phase flow of incompressible hot water in porous aquifer is assumed to follow the Darcy's law:

$$u_w = -\frac{k}{\mu_w}(\nabla p + \rho_w g \nabla z) \tag{3}$$

where μ_w is the dynamic viscosity of water, Pa·s; p denotes the pore pressure within aquifer, Pa; g is the gravitational force, m/s^2; z is the formation depth, m; ∇z is the unit vector in z direction.

The transient heat transfer within the pore space mainly takes place by conduction and convection, and the governing equations for the energy conservation in terms of temperature can be formulated based on the local thermal non-equilibrium theory and descripted as:

$$c_{p,s}\rho_s \frac{\partial}{\partial t}[(1-\phi)T_s] = h(T_w - T_s) + \nabla\cdot[(1-\phi)\lambda_s \nabla T_s] + (1-\phi)Q_w \tag{4}$$

$$c_{p,w}\frac{\partial}{\partial t}(\phi\rho_w T_w) + c_{p,w}\rho_w u_w \cdot \nabla T_w = h(T_w - T_s) + \nabla\cdot(\phi\lambda_w \nabla T_w) + \phi Q_w \tag{5}$$

where T_w and T_s denote the temperature of water and rock mass, K; ρ_s denote the density for rock matrix, kg/m^3; $c_{p,w}$ and $c_{p,s}$ denote the specific heat capacity for water and rock mass, J/(kg·K); λ_w and λ_s denote the thermal conductivity of water and rock; Q_w denotes the heat source term, W·m^{-2}; h denotes the convective heat transfer coefficient, W/(m^3·K).

The physical properties of formation rock are assumed to be independent of temperature and pressure, and the anisotropy of thermal conductivity for rock is neglected in this study (He et al., 2023). In addition, the thermophysical properties of circulating water incorporated in Eqs. (2)-(5) are temperature dependent, the values of which at formation pressure and different temperature conditions are obtained from the NIST (National Institute of Standards and Technology) Chemistry WebBook, SRD 69, as shown in Fig. 2.

The coupled fluid flow and heat transfer problems with above governing equations are solved by using the finite element method. The computation domain is discretized by utilizing the triangular prism mesh scheme, and the boundary of injection and production wells are defined by using rectangular units. The vicinity of the wellbore is discretized by refined mesh to capture the flow and heat transfer behavior. The detailed mesh scheme is given in Fig. 3, which includes 27,440 prisms, 5,488 triangulars, 1,240 quadrilaterals, 368 edges, and 24 vertex elements.

2.3 Initial and boundary conditions

To minimize the boundary effect, a 200 m long and 200 m wide domain is utilized for all numerical simulation scenarios. The porous aquifer is assumed to be confined with no heat and fluid exchange through the top and bottom boundaries, and all side boundaries are assumed to be closed to fluid flow. There is no heat source at the bottom of the aquifer. A typical doublet well system with vertical injection and production wells (as sketched in Fig. 3) is adopted to achieve hot water circulation in the subsurface, and the injection and production wells fully

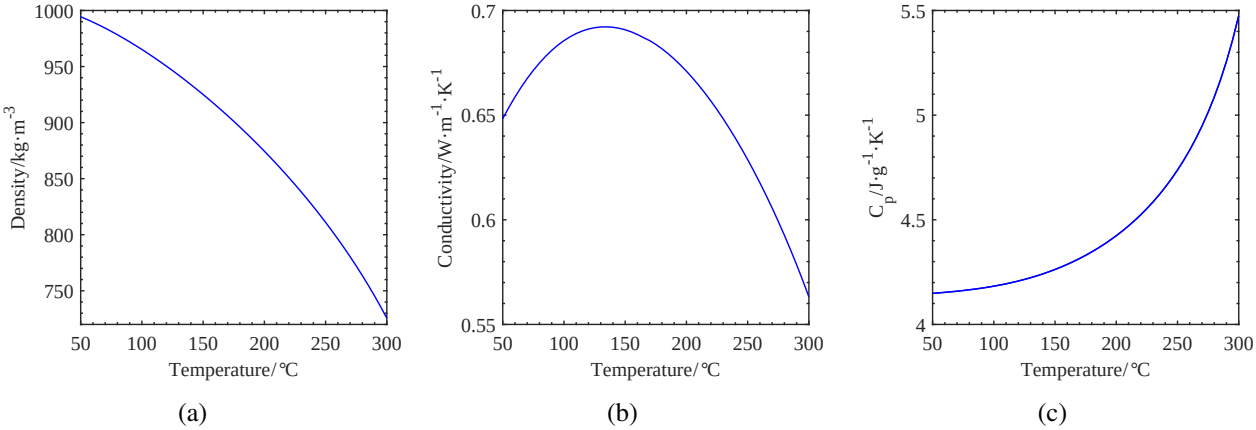

Fig. 2. Variation of (a) density, (b) conductivity and (c) heat capacity of water with temperature in the numerical model.

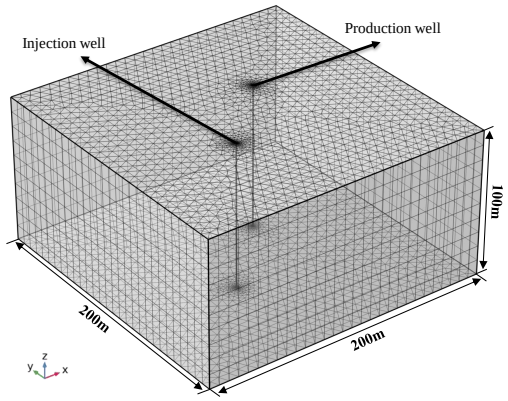

Fig. 3. Illustration of the doublet vertical well system for solar energy storage in deep aquifer and mesh schemes adopted for the whole computation domain.

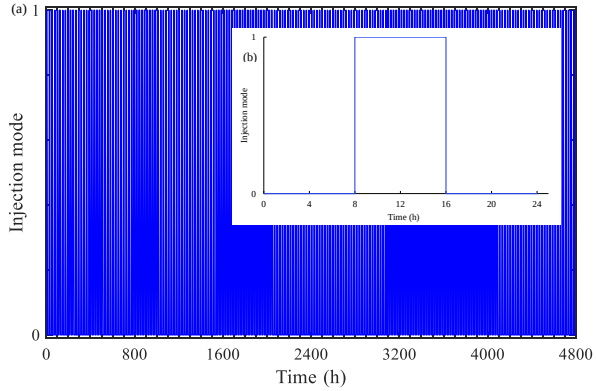

Fig. 4. Schematic illustration of the injection mode for whole hot water circulation process (a) and one day (b): 1 represents an open well status and 0 represents a shut-in well status.

penetrate the formation thickness, and the distance between the two wells is of 70.71 m. The cycling water is assumed be heated through a solar energy collector (e.g., parabolic trough) to 250 °C on the surface and then injected into the aquifer to heat the formation rock and fluids, while the cold water in the subsurface is driven to the producer via injected hot fluids. The injection rate of hot water is about 1,600 m^3/day, and the production well is constrained by a constant bottomhole pressure of 15 MPa. The produced water can be heated again on the surface and then reinjected into the aquifer. To mimic the intermittent heating process by solar energy, the injection of hot water is performed at daytime with an injection rate of 200 m^3/h, which lasts 8 hours per day, and then the injection well is shut-in in the remaining 16 hours (as shown in Fig. 4). The whole thermal energy storage process lasts for 200 days, which stands for the storage phase in the first operation cycle.

The initial temperature and pore pressure of the aquifer are dependent on formation depth. The reference temperature at a depth of 1,500 m is set as 60 °C, with a thermal gradient of 38.5 °C/km. The pore pressure at a reference depth of 1,500 m is set to 15 MPa, with a hydraulic gradient of 10 kPa/m. The targeted deep aquifer is assumed to be fully saturated with formation water at the initial condition. It should be noted that, during the circulation of hot water in the subsurface, the injected hot water remains in a liquid state under the operation pressure conditions.

2.4 Numerical model setup

To explore the feasibility of solar energy storage in deep aquifer, a series of synthetic aquifer models is constructed with different permeability distributions. The average permeability (k_{avg}), dimensionless horizontal autocorrelation length (λ_{Dh}), global permeability heterogeneity in terms of V_{DP}, permeability anisotropy in terms of horizontal to vertical permeability ratio (k_v/k_h), injection rate (V_{inj}) and injection temperature (T_{inj}) are given in Table 1. The physical and thermophysical properties of formation rock and water are given in Table 2.

3. Results and discussion

The performance of thermal energy storage in deep aquifer via hot water circulation is evaluated by using the following metrics. Thermal breakthrough time reflects the time required for the hot front of injected hot water to penetrate the production well, and it is a crucial parameter to assess the sustain-

Table 1. Parameter values for synthetic aquifer models adopted in the simulations.

No.	k_{avg} (mD)	λ_{Dh}	V_{DP}	k_v/k_h	V_{inj} (m^3/h)	T_{inj} (°C)	Gravity
1	100	0	0	1	200	250	No
2	100	0	0	1	200	250	Yes
3	100	0	0	0.1	200	250	Yes
4	100	0	0	1	100	250	Yes
5	100	0	0	1	150	250	Yes
6	100	0	0	1	200	150	Yes
7	100	0	0	1	200	200	Yes
8	50	0	0	1	200	250	Yes
9	200	0	0	1	200	250	Yes
10	100	0	0.63	1	200	250	Yes
11	100	0.2	0.63	1	200	250	Yes
12	100	0.5	0.63	1	200	250	Yes
13	100	0.5	0.39	1	200	250	Yes
14	100	0.5	0.78	1	200	250	Yes

ability of the aquifer. For porous aquifer, the thermal breakthrough time is referred to the time for 10% thermal buildup (TB), which can be calculated as the increase ratio of the produced water temperature during solar energy storage process (Zhang et al., 2023):

$$\mathrm{TB} = \frac{T_{prod} - T_{ini}}{T_{inj} - T_{ini}} \tag{6}$$

where T_{prod} is the temperature of produced water, °C; T_{inj} denotes the temperature of injected water, °C; T_{ini} is the initial temperature of the aquifer, °C.

The cumulative heat stored in the aquifer is applied to evaluate the overall solar energy storage performance in deep aquifer, which can be expressed as the cumulative heat injected into the aquifer minus the cumulative heat carried out by produced water:

$$Q_s = Q_{inj} - Q_{prod} \tag{7}$$

where Q_s is the cumulative heat stored in the aquifer, TJ; Q_{inj} is the cumulative heat injected into the aquifer, TJ; Q_{prod} is the cumulative heat carried out by produced water, TJ.

The bottomhole pressure of injection well is also adopted to assess the feasibility of hot water circulation implementation in field operation.

3.1 Influence of buoyancy-driven flow

During the circulation of hot water in the aquifer, apparent density difference exists due to the large temperature gradient between injected water and in-situ formation water, which can arouse a buoyancy-driven flow in the subsurface. To elucidate the impact of buoyancy-driven flow of hot water on thermal energy storage process, heat storage simulations are carried out by using a homogeneous aquifer with and without consideration of gravitational force. Fig. 5 presents the temporal and spatial evolution of the hot water zone between injection and production wells under different conditions. It can be observed that, the high temperature region induced by injected hot water gradually expands towards the production well with the proceeding of heat storage, indicating that the heat injected into the aquifer is gradually stored. Without considering gravity, an even hot water front along vertical direction can be obtained over whole operation process, and a preferably large heated volume can be obtained at the end of circulation, which implies that the heat storage capacity of the aquifer can be efficiently utilized. However, with the consideration of gravity, the hot water zone presents a cone shape with the action of gravity override, and the lower part of the aquifer has not been swept by hot water at the end of operation. This phenomenon demonstrates that the heat storage capacity in the lower region of the aquifer may not be effectively utilized affected by buoyancy-driven flow, and thus the amount of thermal energy trapped in the aquifer is reduced. In addition, it can be inferred that the adverse impact of buoyancy-driven flow on heat storage performance may be exaggerated with the increasing thickness of aquifer, whilst this effect of buoyant force may be reduced when storing heat within high anisotropic and/or thin layered aquifers. Also, the phenomenon of buoyancy-driven flow may cause some trouble when the heat is tapped from the aquifer by cold water circulation, because in such condition, cold water injected tends to migrate in the lower part of the aquifer.

Table 2. General model parameters for a base case design.

Properties	Value
Mean porosity (fraction)	0.23
Averaged permeability (mD)	100
Density of formation rock (kg/m^3)	2,700
Thermal conductivity of rock (W/(m·K))	3
Convective heat transfer coefficient ($W/(m^3 \cdot K)$)	10
Specific heat capacity of rock ($J \cdot kg^{-1} \cdot K^{-1}$)	1,000
Density of water@250 °C (kg/m^3)	811.03
Thermal conductivity of water@250 °C (W/(m·K))	0.63
Specific heat capacity of water@250°C ($J \cdot kg^{-1} \cdot K^{-1}$)	4,738
Temperature of injection fluids (°C)	250
Injection rate (kg/s)	45.06
Reference temperature of aquifer (°C)	60
Reference pressure of aquifer (MPa)	15
Borehole diameter (cm)	10

The change of produced water temperature over the whole 200 days operation period for different simulation schemes is illustrated in Fig. 6. It can be clearly seen that, without the consideration of gravity, the temperature of produced water remains at the initial ambient temperature of 60 °C in the first 140 days of hot water circulation. The reason behind this is that the hot front of the injected water has not arrived at

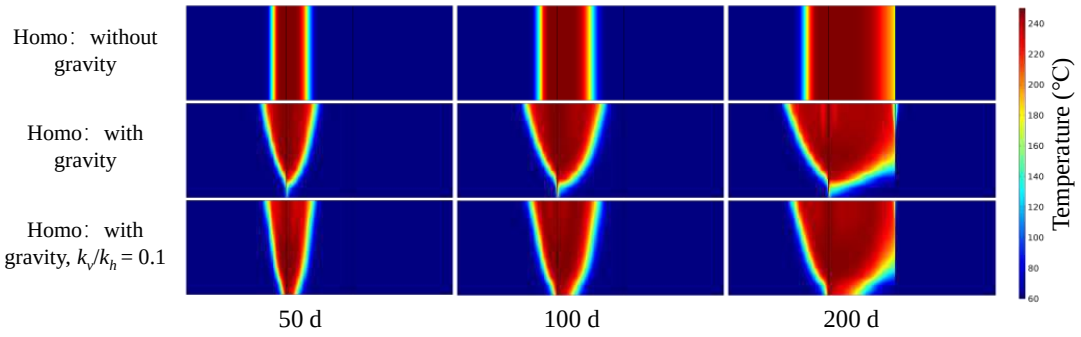

(a)

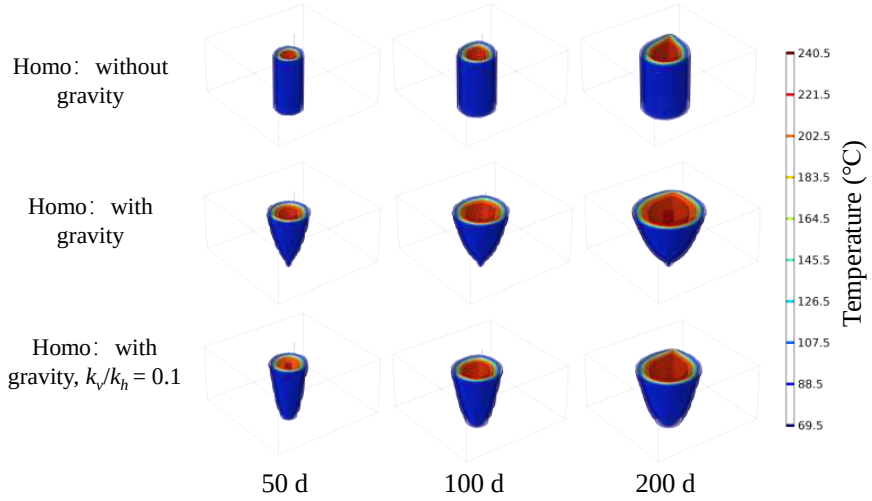

(b)

Fig. 5. Temporal and spatial evolution of hot water zone in the aquifer for cases without gravity, with gravity, and under anisotropic condition: (a) temperature profile between injection and production wells, (b) 3D temperature field. A homogeneous model with permeability of 100 mD is adopted for all the cases.

the production well in the first 140 days of operation and hence the region near the production well keeps almost no changes and maintains at the ambient formation temperature of 60 °C. As the hot front of the injection water penetrates the production well after 140 days, the temperature of produced water begins to rise gradually. According to the simulation results, the temperature of produced water is elevated to 100 °C at the end of operation. Compared with the case without the consideration of gravity, the thermal breakthrough time is approximately shortened by 14.2 days for the case considering gravity, and the temperature of produced water fluctuates slightly after thermal breakthrough. The reason behind this is that the injected hot water tends to ascend vertically under the action of buoyant force, which alters the shape of hot water zone. As the thermal front approaches the production well successively, the temperature of produced water increases continuously but fluctuates to a certain extent.

The cumulative heat stored in aquifer under different scenarios are compared, as shown in Fig. 7. The amount of thermal energy stored in the aquifer without gravity is up to 213.74 TJ (i.e., 5.94×10^4 MWh_t) after 200 days of circulation, with 30% contained in formation water, and 70% stored in rock mass. As can be seen from Fig. 7, compared with the scenario without gravity, the cumulative heat stored in aquifer for the case considering gravity is lowered from 213.74 to 211.76 TJ. Therefore, the buoyancy-driven flow can impose a negative effect on heat storage efficiency. However, as for an anisotropic aquifer with k_v/k_h of 0.1, the produced water temperature at the end of operation is reduced by 5 °C compared with isotropic condition (see Fig. 6), and the cumulative heat stored is effectively improved to 213.25 TJ.

The variation of bottomhole pressure of the injection well over whole operation period is shown in Fig. S1. The bottomhole pressure declines gradually with the proceeding of heat storage in the subsurface, and meanwhile a certain degree of fluctuation can be observed, which can be attributed to the repeated well opening and closing operations. The difference in bottomhole pressure is not obvious for cases with and without consideration of gravity. However, the operation pressure for hot water injection into heterogeneous aquifer is obviously higher than that of homogeneous aquifer. An unwilling elevation of injection pressure may cause some trou-

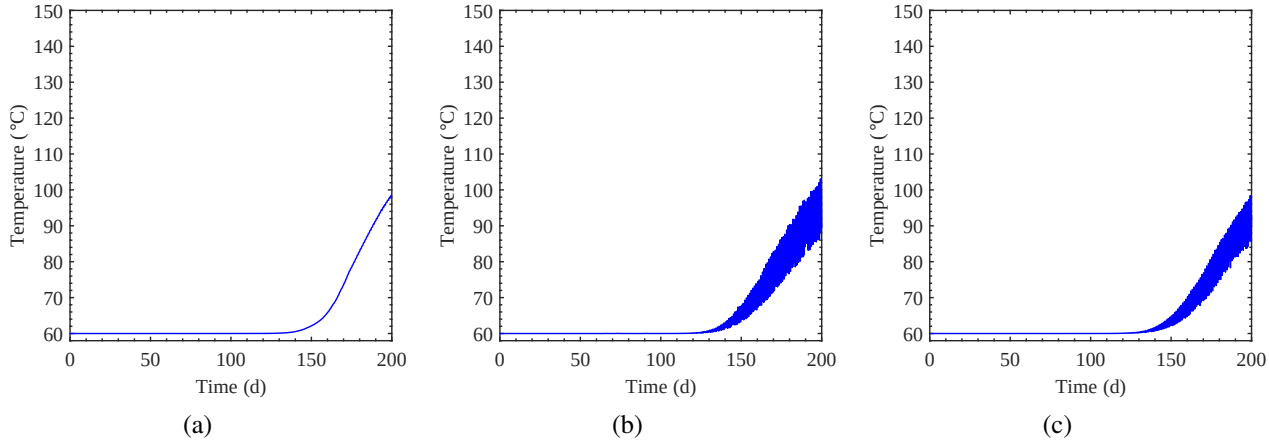

Fig. 6. Temperature of produced water during whole hot water circulation process for different homogeneous cases (a) without gravity, (b) with gravity and (c) with gravity, k_v/k_h = 0.1.

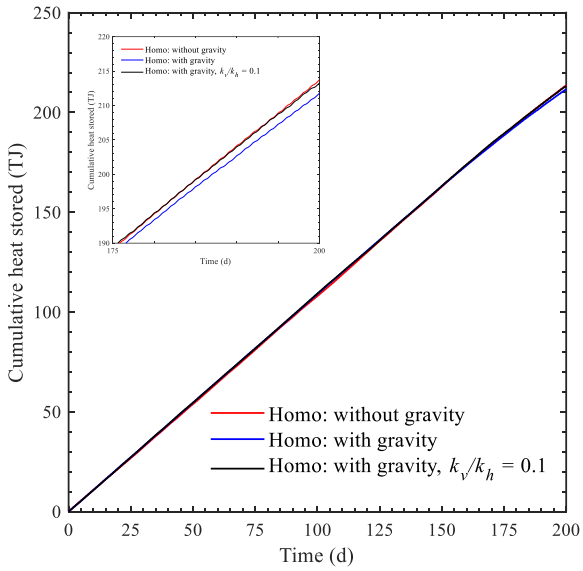

Fig. 7. Evolution of cumulative heat stored in aquifer under different scenarios.

ble for field operation and increase the operation costs.

3.2 Influence of injection conditions

Temporal and spatial evolution of hot water zone in the aquifer for cases with different injection rates are shown in Fig. 8. It can be observed that the increase of the injection rate increases the swept volume of hot water, and thus enlarges the heat stored in aquifer. However, as shown in Fig. 9, the increase of injection rate accelerates the breakthrough of hot water into production well and elevates the operation pressure (Fig. S2).

The influence of injection temperature on heat storage process in deep aquifer is investigated and the simulation results are shown in Figs. 10 and 11. From the temporal and spatial evolution of hot water zone (Fig. 10), the temperature of hot water zone can be significantly promoted when the injection temperature is 250 °C, which means much more heat can be stored in the subsurface. In addition, the increase of injection temperature can shorten the thermal breakthrough time (Fig. 11), but cause negligible effect on injection pressure (Fig. S3).

3.3 Influence of average permeability

The effect of average permeability of aquifer on heat storage performance has been studied, and the temporal and spatial evolution of the hot water zone in aquifer is given in Fig. 12. It can be seen that, the increase of permeability may promote the gravity override effect of hot water, and a high injection pressure can be encountered for aquifer with permeability of 50 mD (Fig. S5). The results indicate that deep aquifers with moderate permeabilities are more preferred and should be chosen in field operation to reduce the negative effects of low injectivity (for low permeability aquifer) and gravity override (for high permeability aquifer).

3.4 Influence of permeability heterogeneity

3.4.1 Horizontal autocorrelation length

The aforementioned results show that buoyancy-driven flow mainly affects the expansion process of hot water zone in aquifer and reduces the swept volume of hot water in the lower part of the aquifer, which in turn deteriorates heat storage performance. In general, deep aquifers are usually featured with heterogeneous permeability, and thus spatial heterogeneity will further change the flow pathways of hot water in the subsurface. This part aims to explore the influence of horizontal correlation length of permeability fields on heat storage performance. To achieve this, three typical synthetic permeability distributions with different horizontal autocorrelation length and the same vertical autocorrelation length of 0 and V_{DP} of 0.63 are generated.

The evolution of temperature distribution under different horizontal autocorrelation length scenarios is presented in Fig. 13. The temporal and spatial distributions of hot water zone at

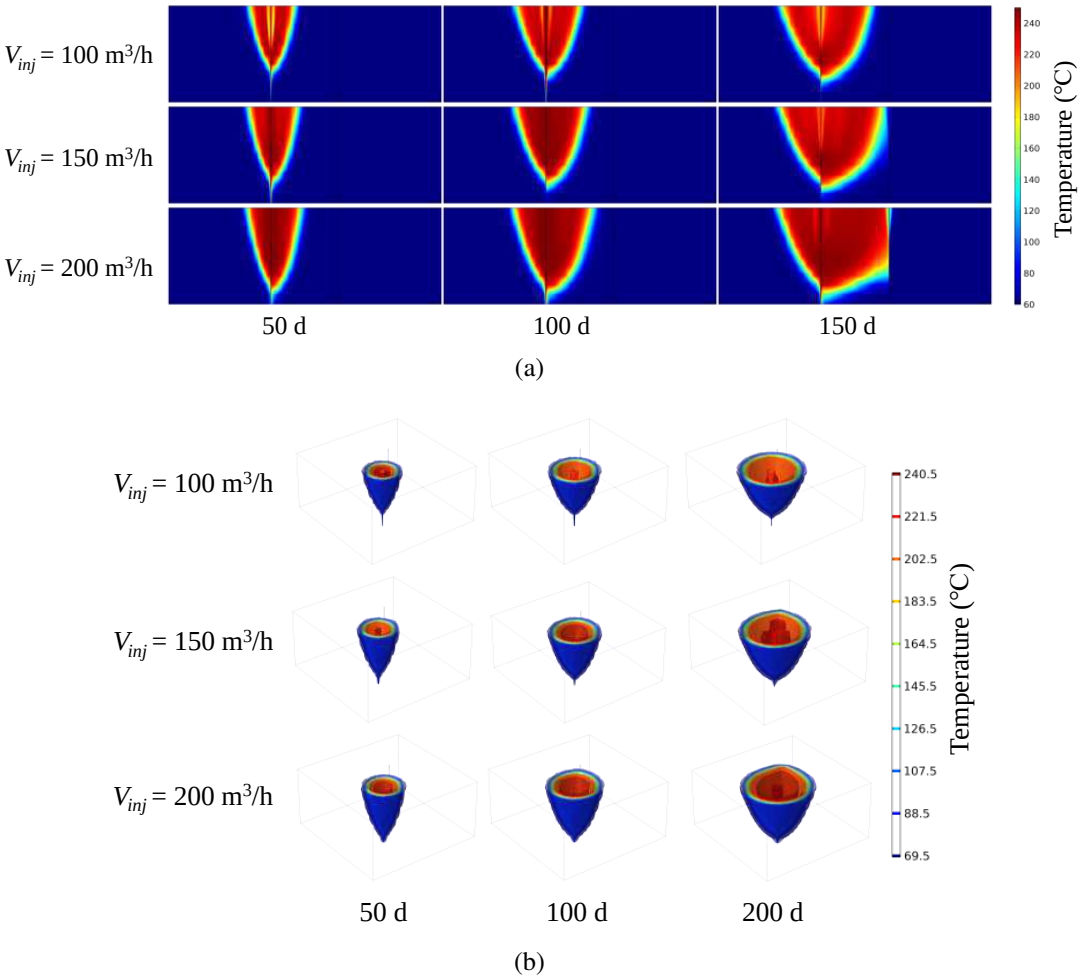

Fig. 8. Temporal and spatial evolution of hot water zone in the aquifer for cases with V_{inj} = 100 m³/h, V_{inj} = 150 m³/h and V_{inj} = 200 m³/h: (a) temperature profile between injection and production wells and (b) 3D temperature field.

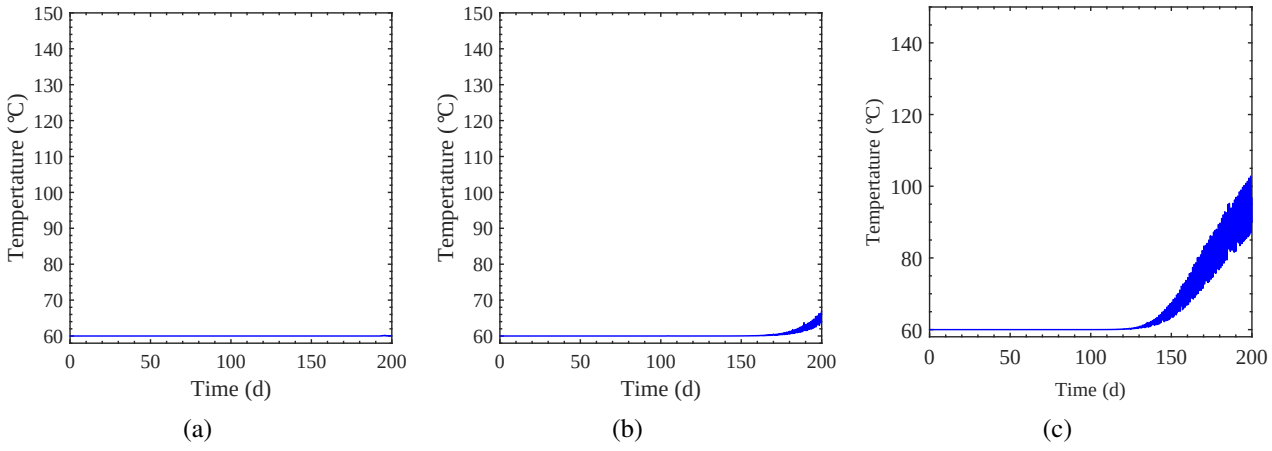

Fig. 9. Evolution of produced water temperature over whole circulation process with (a) V_{inj} = 100 m³/h, (b) V_{inj} = 150 m³/h and (c) V_{inj} = 200 m³/h.

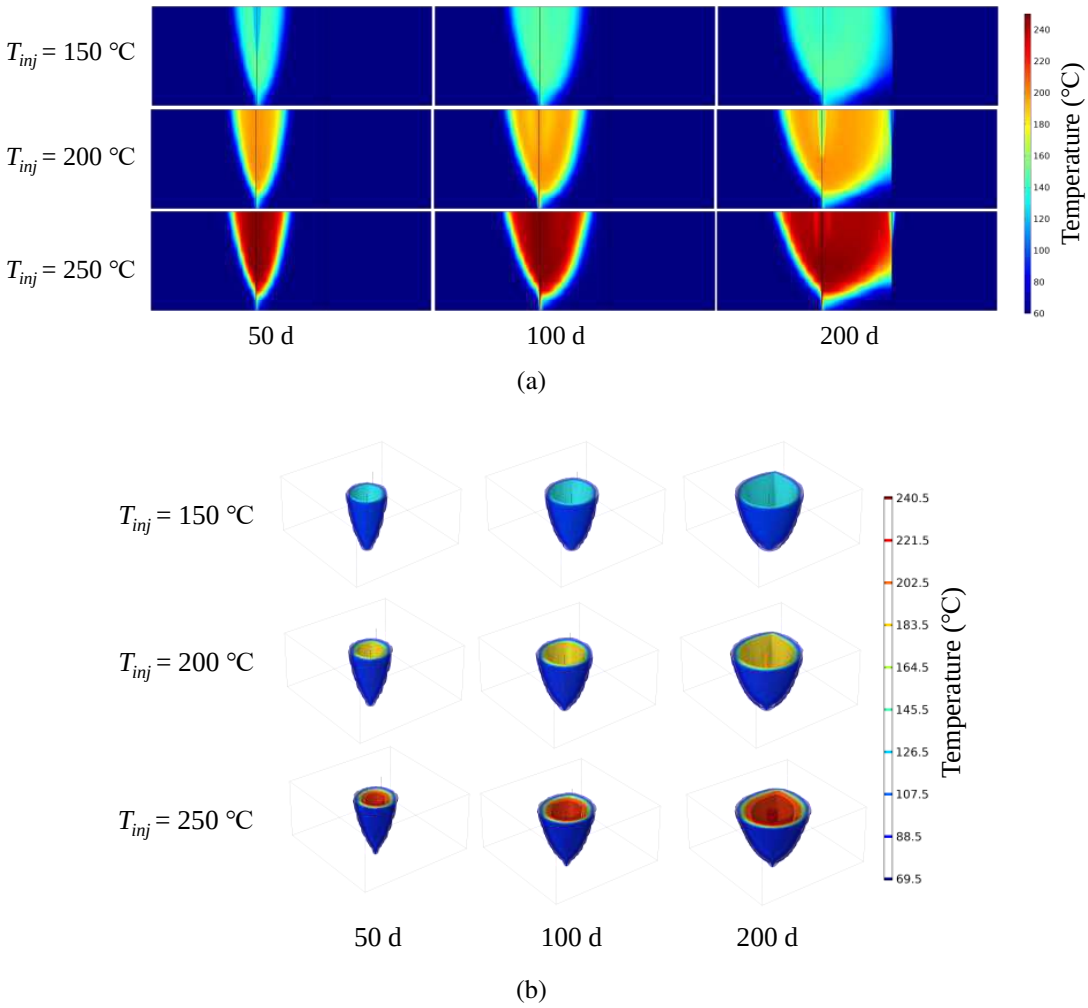

Fig. 10. Temporal and spatial evolution of hot water zone in the aquifer for cases with T_{inj} = 150 °C, T_{inj} = 200 °C and T_{inj} = 250 °C: (a) temperature profile between injection and production wells, (b) 3D temperature field.

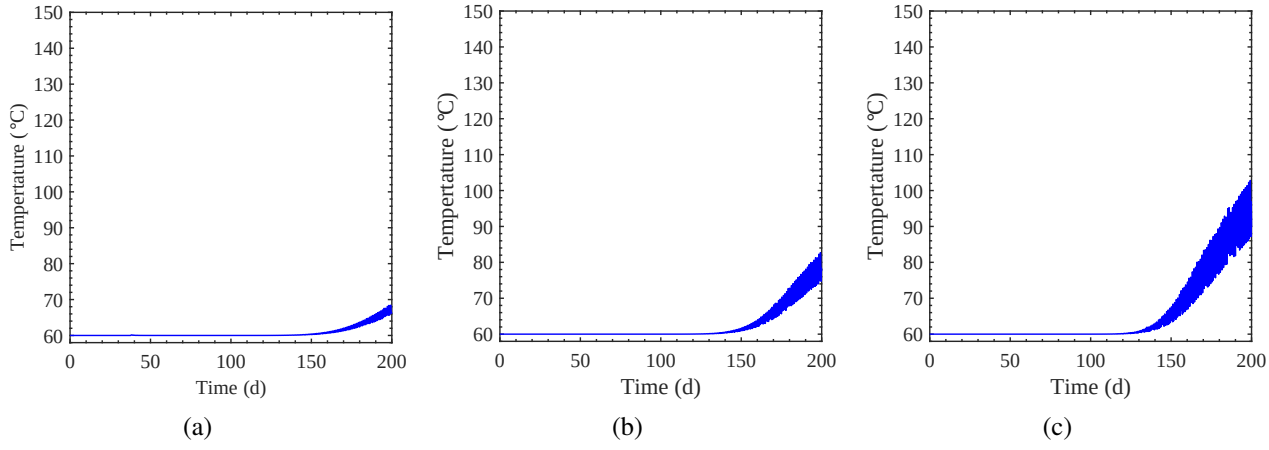

Fig. 11. Evolution of produced water temperature over whole circulation process ith (a) T_{inj}=150 °C, (b) T_{inj}=200 °C and (c) T_{inj}=250 °C.

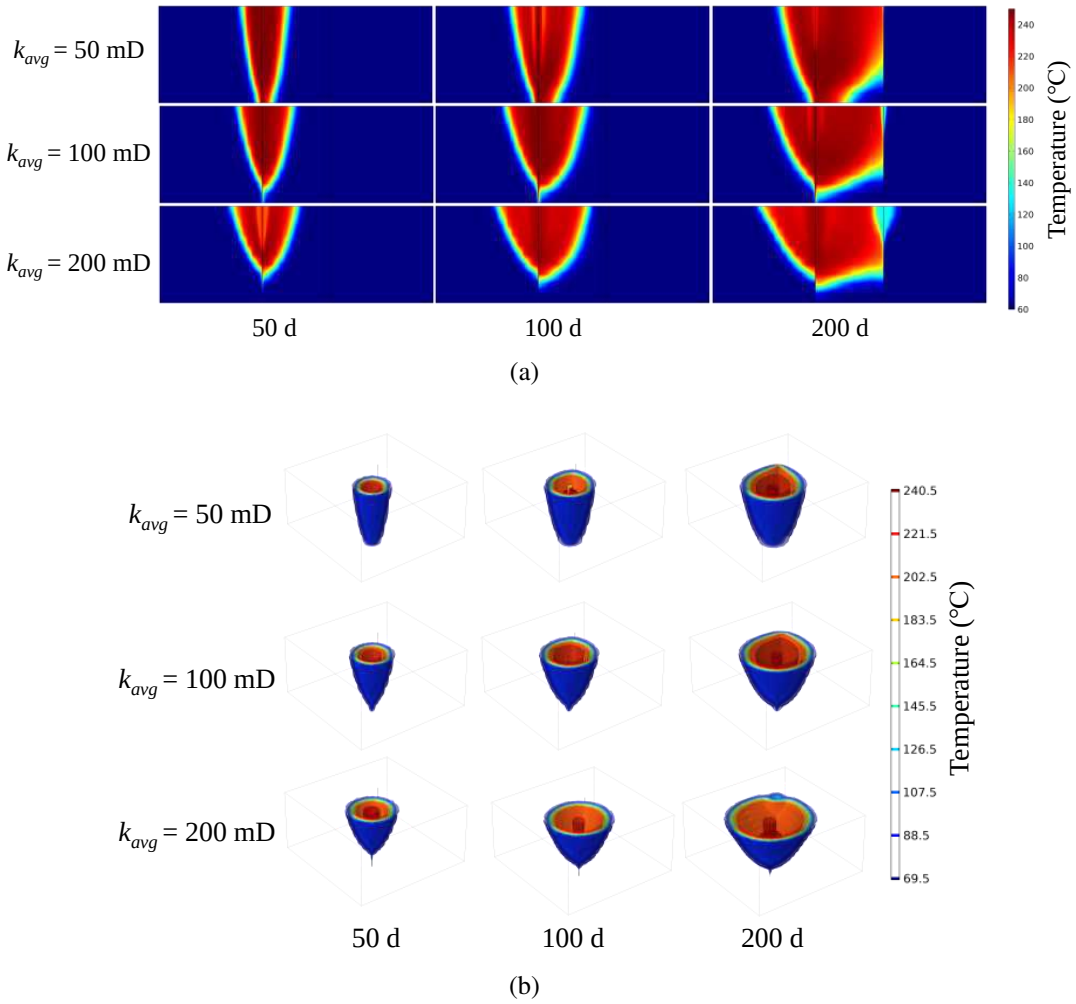

Fig. 12. Temporal and spatial evolution of hot water zone in the aquifer for cases with k_{avg} = 50 mD, k_{avg} = 100 mD and k_{avg} = 200 mD: (a) temperature profile between injection and production wells and (b) 3D temperature field.

different simulation times for the heterogeneous scenario show that, non-uniform thermal front is formed with the gradual expansion of high temperature region. The reason behind this is that preferential flow pathways exist in the heterogeneous permeability fields, and thus the migration of hot water in the subsurface is synergistically dominated by buoyancy-driven flow and channeling flow. As a result, the lower part of the aquifer near the production well cannot be effectively heated at the end of circulation, which means a portion of heat storage capacity cannot be effectively utilized and amount of thermal energy stored in subsurface will be reduced. It can also be seen that a relatively smooth high temperature front can be obtained during hot water circulation in deep aquifer featured with uncorrelated permeability field. The increase of horizontal autocorrelation length obviously accelerates the penetration of hot water into production well. The swept volume of hot water is also diminished, which means the quantity of thermal energy stored in subsurface decreases. As can be seen from Fig. 13, the temperature of the upper region near the production well is obviously lower than that of the middle region, which illustrates that the channeling flow of hot water overwhelms its buoyancy-driven flow. The reason behind this is that with increasing horizontal autocorrelation length, preferential flow pathway may appear between injection and production wells, and the hot water injected tends to migrates along the high permeability channels. In such condition, the channeling flow through high permeability zones makes up for the majority of the produced water.

In comparison to a homogeneous aquifer, it can be seen from Fig. 14 that the thermal breakthrough time is further shortened to 134.2 days from 146.2 days during hot water circulation in an uncorrelated heterogeneous aquifer (with horizontal autocorrelation length of 0, and V_{DP} of 0.63). This indicates that spatial distribution of permeability can strongly affect the heat storage potential in aquifer. One can also see that, for an aquifer featured with uncorrelated permeability field, the temperature of produced water rises gradually from 60 to 95 °C after the thermal breakthrough, featured with a small level of fluctuation. As dimensionless horizontal autocorrelation length increases from 0 to 0.5, the thermal breakthrough time reduces from 134.2 to 70.2 days, and

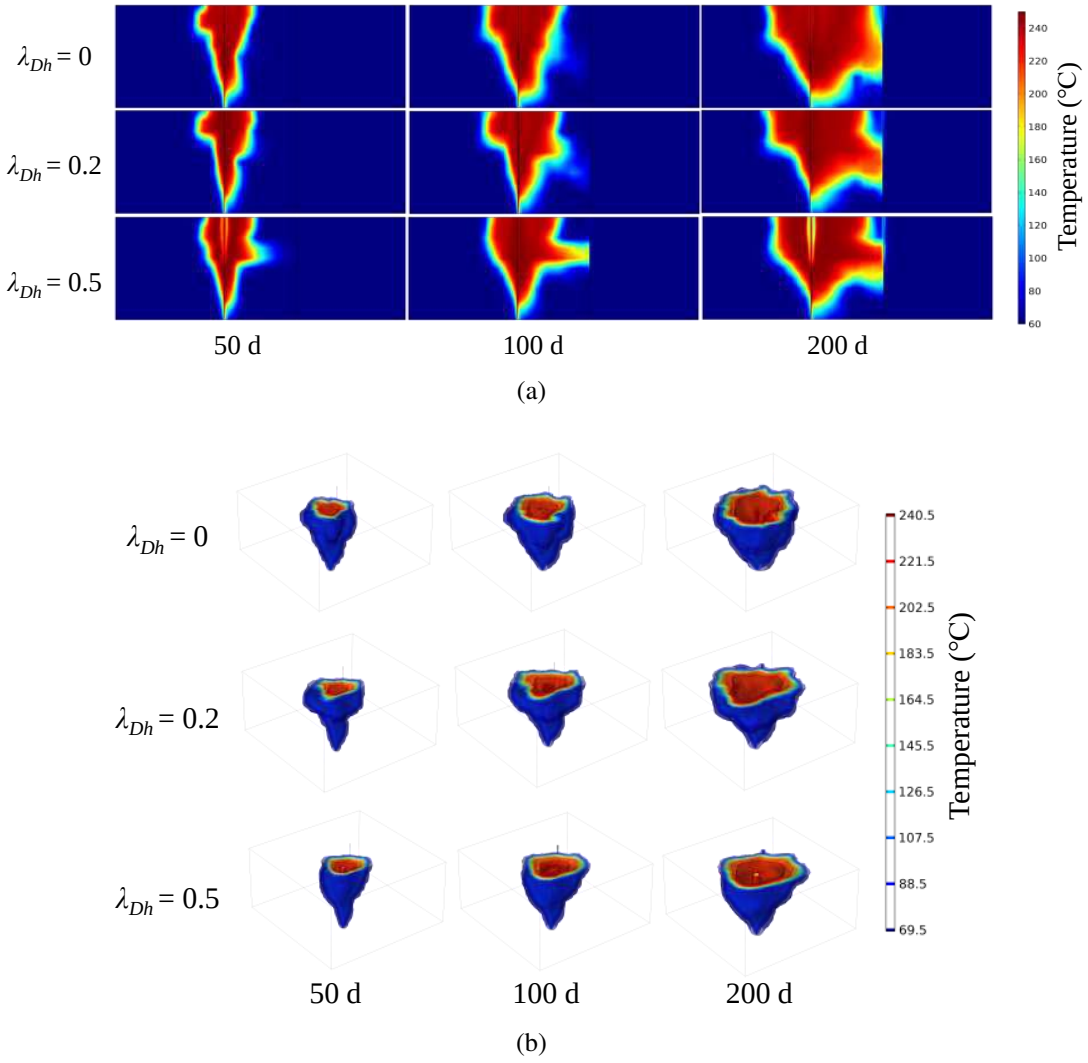

Fig. 13. Temporal and spatial evolution of hot water zone in the aquifer for cases with λ_{Dh} = 0, λ_{Dh} = 0.2 and λ_{Dh} = 0.5: (a) temperature profile between injection and production wells and (b) 3D temperature field.

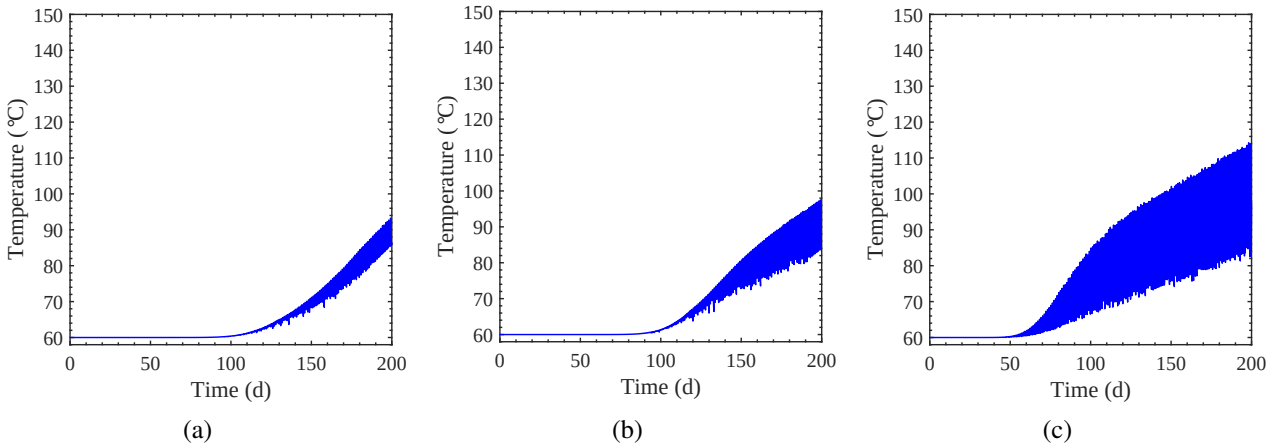

Fig. 14. Evolution of produced water temperature over whole circulation process with (a) λ_{Dh} = 0, (b) λ_{Dh} = 0.2 and (c) λ_{Dh} = 0.5. The average permeability for all cases equals 100 mD, vertical autocorrelation length equals 0, and V_{DP} equals 0.63.

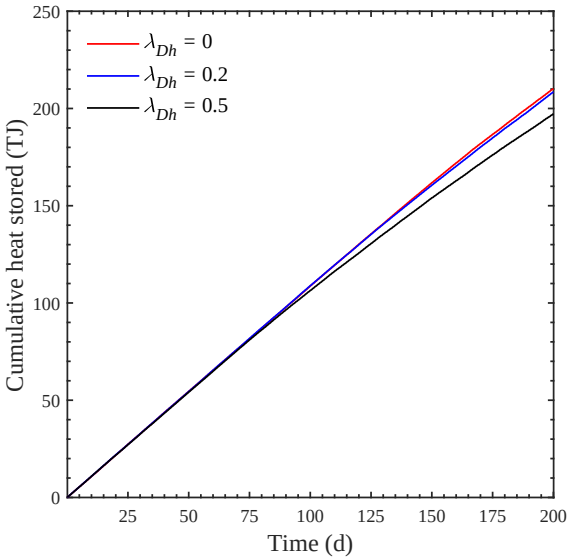

Fig. 15. Evolution of cumulative heat stored in aquifer under different horizontal autocorrelation length scenarios.

the temperature of produced water at the end of operation increases from 95 to 115 °C, with an enlarged fluctuation of produced water temperature. The reason behind this is that preferential flow pathway may be present between the injection and production wells, which can significantly enhance the lateral movement of hot water and shorten the thermal breakthrough time. Fig. 15 gives the cumulative heat stored in the aquifer with the proceeding of hot water circulation. The total heat stored in aquifer at the end of circulation is reduced from 210.25 to 197.29 TJ with λ_{Dh} increasing from 0 to 0.5, which demonstrates that the effective heat storage capacity of the aquifer can be deteriorated with the increase of horizontal autocorrelation length.

The bottomhole pressure of injection well over whole circulation process is given in Fig. S6. No noticeable variation of injection pressure is observed with the increase of horizontal correlation length. From the point view of heat storage quantity and efficiency, porous aquifers featured with smaller autocorrelation length will be more favored and suggested to be selected prior to field operation.

3.4.2 Global permeability heterogeneity

In addition to correlation length, global permeability heterogeneity (in terms of V_{DP}) can also impose a significant impact on spatial heterogeneity of subsurface aquifer. To clarify the effect of global permeability heterogeneity on heat storage performance, three permeability fields are generated with typical values of V_{DP} and the same autocorrelation length. The horizontal and vertical autocorrelation lengths for all permeability fields are set to 0.5 and 0, respectively. Fig. 16 presents the temporal and spatial evolution of hot water zone across circulation well system under different global permeability heterogeneity conditions. It can be clearly seen from Fig. 16 that the expansion of hot water zone is very sensitive to global permeability heterogeneity. With the same autocorrelation length, the increase of global permeability heterogeneity significantly promotes the channeling of hot water into production well along the preferential flow pathways, which finally deteriorates the thermal energy storage quantity and efficiency.

The change of produced water temperature during hot water circulation process is presented in Fig. 17. It can be seen that, the thermal breakthrough time is reduced from 113.2 days to 40.2 days with V_{DP} increasing from 0.39 to 0.78, and the temperature of produced water at the end of operation increases from 115 to 140 °C. After the breakthrough of thermal front into production well, a violent fluctuation of temperature can be observed, especially for the case with V_{DP} of 0.78. Earlier breakthrough of thermal front into production well finally results in an inefficient circulation of hot water in the subsurface and worsens the thermal energy storage performance. Fig. 18 presents the cumulative heat stored in aquifer under different global permeability heterogeneity conditions. As shown in Fig. 18, the total heat stored at the end of circulation decreases by 11.62% from 204.54 to 180.77 TJ, with V_{DP} increasing from 0.39 to 0.78. The evolution of injection pressure over the whole circulation process is shown in Fig. S7. One can see that the enhancement of global permeability heterogeneity obviously elevates the injection pressure for hot water injection, which means additional operation costs will be required in field application.

4. Conclusions

In this work, geostatistical method and coupled hydro-thermo modeling are used to assess the feasibility of storing solar thermal energy in deep heterogeneous aquifers through a doublet well system. Specifically, the impacts of buoyancy-driven flow and spatial permeability heterogeneity (i.e., horizontal autocorrelation length and global permeability variation) on the performance of thermal energy storage are illustrated. The key findings are as follows:

1) Converting and storing solar thermal energy as deep aquifer heat through hot water circulation is a viable approach. Under typical operational conditions (i.e., injection temperature of 250 °C, injection rate of 1,600 m^3/d), the cumulative thermal energy stored in a heterogeneous aquifer (with λ_{Dh} = 0, V_{DP} = 0.63) can reach up to 210.25 TJ (i.e., 5.84×10^4 MWh_t) after 200 days of circulation.
2) During the circulation of hot water in aquifer, buoyant-driven flow limit water sweep in the lower part of the aquifer, reducing thermal energy storage quantity by 0.93% in the simulation condition.
3) The increase in horizontal autocorrelation length and permeability heterogeneity may accelerate thermal breakthrough and reduce thermal storage quantity. Highly heterogeneous aquifers also increase well injection pressure. Thus, regarding heat storage site selection, deep aquifers with a moderate average permeability, smaller horizontal autocorrelation lengths and less global heterogeneity are preferred for efficient and cost-effective storage. In field applications, optimized flow and heat transfer control may further improve field-scale storage capacity.

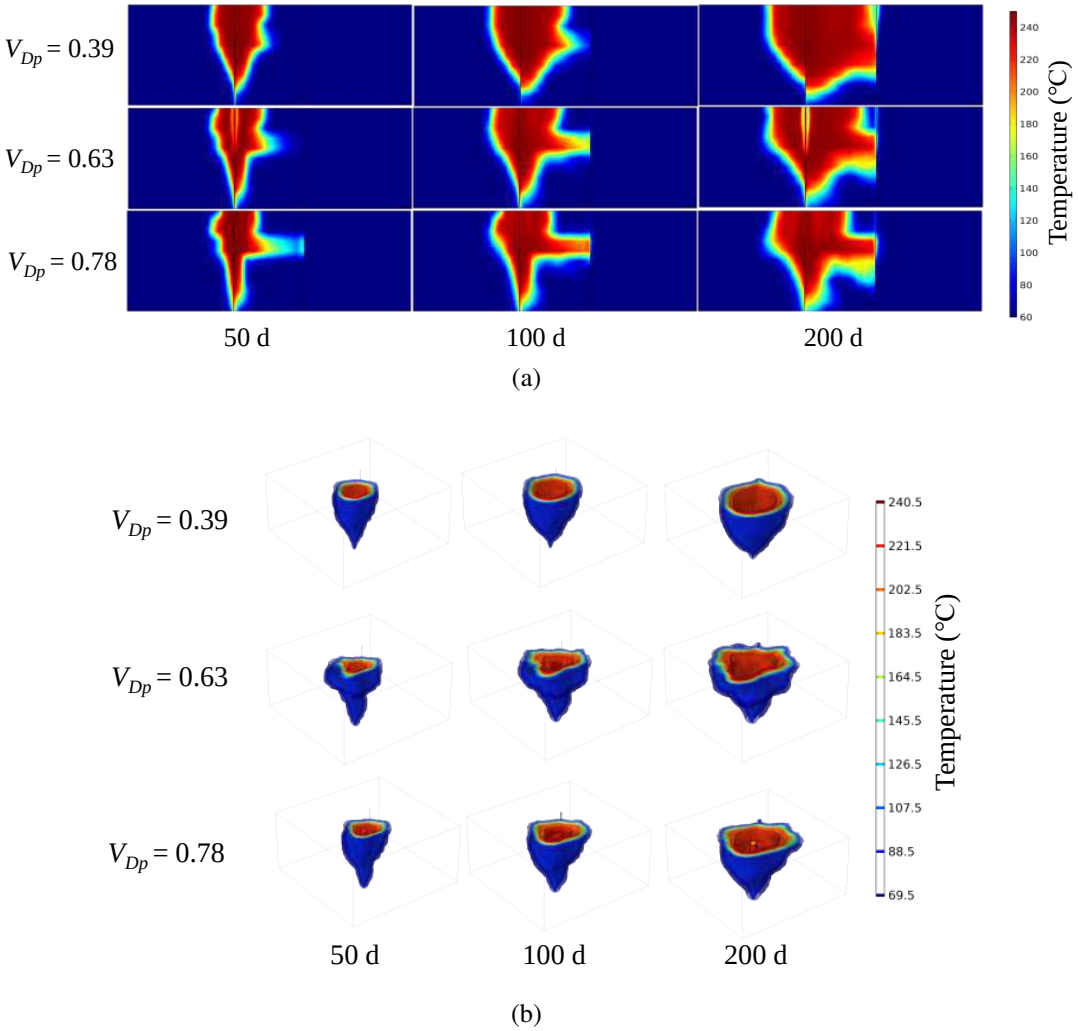

Fig. 16. Temporal and spatial evolution of hot water zone in the aquifer for cases with V_{Dp} = 0.39, V_{Dp} = 0.63 and V_{Dp} = 0.78: (a) temperature profile between injection and production wells, (b) 3D temperature field.

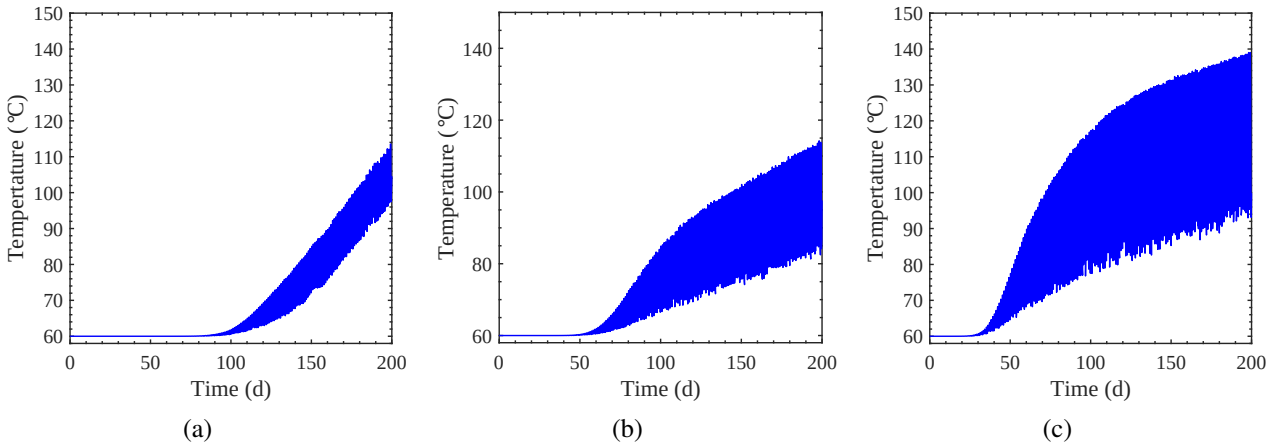

Fig. 17. Evolution of produced water temperature over whole circulation process with (a) V_{DP} = 0.39, (b) V_{DP} = 0.63 and (c) V_{DP} = 0.78. The horizontal autocorrelation length for all cases equal 0.5, and average permeability equals 100 mD.

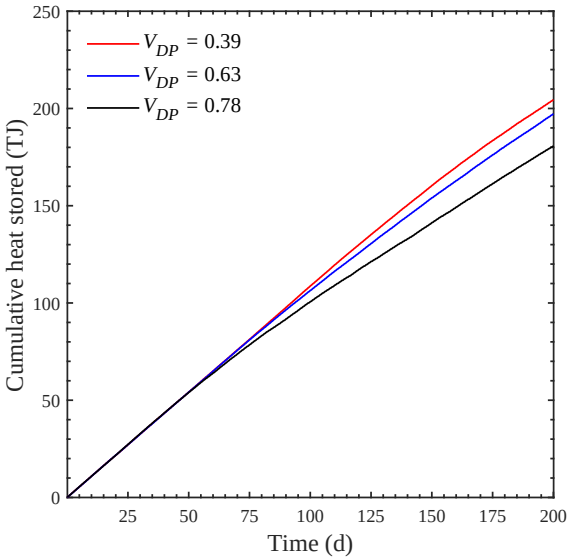

Fig. 18. Evolution of cumulative heat stored in the aquifer under different V_{DP} scenarios.

Acknowledgements

The authors are grateful for the financial support by National Natural Science Foundation of China (No. 52192622), Sichuan Science and Technology Program (Nos. 2021ZYCD004 and 2022YFSY0008) and Chengdu University of Technology 2023 Young and Middle-aged Backbone Teachers Development Funding Program (No. 10912-JXGG2023-08522).

Supplementary file

https://doi.org/10.46690/ager.2023.12.03

Conflict of interest

The authors declare no competing interest.

References

Birdsell, D. T., Adams, B. M., Saar, M. O. Minimum transmissivity and optimal well spacing and flow rate for high-temperature aquifer thermal energy storage. Applied Energy, 2021, 289: 116658.

Cui, G., Ning, F., Dou, B., et al. Particle migration and formation damage during geothermal exploitation from weakly consolidated sandstone reservoirs via water and CO_2 recycling. Energy, 2022, 240: 122507.

Deutsch, C. V., Journel, A. G. GSLIB Geostatistical Software Library and User's Guide. New York, USA, Oxford University Press, 1997.

Fleuchaus, P., Schüppler, S., Bloemendal, M., et al. Risk analysis of high-temperature aquifer thermal energy storage (HT-ATES). Renewable and Sustainable Energy Reviews, 2020a, 133: 110153.

Fleuchaus, P., Schüppler, S., Godschalk, B., et al. Performance analysis of aquifer thermal energy storage (ATES). Renewable Energy, 2020b, 146: 1536-1548.

Gao, Q., Li, M., Yu, M., et al. Review of development from GSHP to UTES in China and other countries. Renewable and Sustainable Energy Reviews, 2009, 13(6-7): 1383-1394.

Green, S., McLennan, J., Panja, P., et al. Geothermal battery energy storage. Renewable Energy, 2021, 164: 777-790.

He, J., Wen, L., He, X., et al. Method to measure radial thermal conductivity for cylindrical samples. ACS Omega, 2023, 8(7): 6530-6537.

Holtz, M. H. Residual gas saturation to aquifer influx: A calculation method for 3-D computer reservoir model construction. Paper SPE 75502 Presented at SPE Unconventional Resources Conference/Gas Technology Symposium, Calgary, Alberta, 30 April-2 May, 2002.

Huang, Y., Pang, Z., Kong, Y., et al. Assessment of the high-temperature aquifer thermal energy storage (HT-ATES) potential in naturally fractured geothermal reservoirs with a stochastic discrete fracture network model. Journal of Hydrology, 2021, 603: 127188.

Ijeje, J. J., Gan, Q., Cai, J. Influence of permeability anisotropy on heat transfer and permeability evolution in geothermal reservoir. Advances in Geo-Energy Research, 2019, 3(1): 43-51.

Jello, J., Khan, M., Malkewicz, N., et al. Advanced geothermal energy storage systems by repurposing existing oil and gas wells: A full-scale experimental and numerical investigation. Renewable Energy, 2022, 199: 852-865.

Kastner, O., Norden, B., Klapperer, S., et al. Thermal solar energy storage in Jurassic aquifers in Northeastern Germany: A simulation study. Renewable Energy, 2017, 104: 290-306.

Liu, S., Taleghani, A. D. Analysis of an enhanced closed-loop geothermal system. Geoenergy Science and Engineering, 2023, 231: 212296.

Major, M., Poulsen, S. E., Balling, N. A numerical investigation of combined heat storage and extraction in deep geothermal reservoirs. Geothermal Energy, 2018, 6(1): 1-16.

Panja, P., McLennan, J., Green, S. Influence of permeability anisotropy and layering on geothermal battery energy storage. Geothermics, 2021a, 90: 101998.

Panja, P., McLennan, J., Green, S. Impact of permeability heterogeneity on geothermal battery energy storage. Advances in Geo-Energy Research, 2021b, 5(2): 127-138.

Ricks, W., Norbeck, J., Jenkins, J. The value of in-reservoir energy storage for flexible dispatch of geothermal power. Applied Energy, 2022, 313: 118807.

Shi, Y., Cui, Q., Song, X., et al. Thermal performance of the aquifer thermal energy storage system considering vertical heat losses through aquitards. Renewable Energy, 2023, 207: 447-460.

Shi, Y., Song, X., Wang, G., et al. Study on wellbore fluid flow and heat transfer of a multilateral-well CO_2 enhanced geothermal system. Applied Energy, 2019, 249: 14-27.

Sommer, W., Valstar, J., van Gaans, P., et al. The impact of aquifer heterogeneity on the performance of aquifer thermal energy storage. Water Resources Research, 2013, 49(12): 8128-8138.

Song, X., Li, G., Huang, Z., et al. Review of high-temperature geothermal drilling and exploitation technologies. Gondwana Research, 2023, 122: 315-330.

Wang, Y., Wang, X., Xu, H., et al. Numerical investigation of the influences of geological controlling factors on heat extraction from hydrothermal reservoirs by CO_2 recycling. Energy, 2022, 252: 124026.

Wang, K., Yuan, B., Ji, G., et al. A comprehensive review of geothermal energy extraction and utilization in oilfields. Journal of Petroleum Science and Engineering, 2018, 168: 465-477.

Wesselink, M., Liu, W., Koornneef, J., et al. Conceptual market potential framework of high temperature aquifer thermal energy storage-A case study in the Netherlands. Energy, 2018, 147: 477-489.

Winterleitner, G., Schütz, F., Wenzlaff, C., et al. The impact of reservoir heterogeneities on high-temperature aquifer thermal energy storage systems. A Case Study from Northern Oman. Geothermics, 2018, 74: 150-162.

Xu, T., Yuan, Y., Jia, X., et al. Prospects of power generation from an enhanced geothermal system by water circulation through two horizontal wells: A case study in the Gonghe Basin, Qinghai Province, China. Energy, 2018, 148: 196-207.

Yang, R., Wang, Y., Song, G., et al. Fracturing and thermal extraction optimization methods in enhanced geothermal systems. Advances in Geo-Energy Research, 2023, 9(2): 136-140.

Zhang, L., Cui, G., Zhang, Y., et al. Influence of pore water on the heat mining performance of supercritical CO_2 injected for geothermal development. Journal of CO_2 Utilization, 2016, 16: 287-300.

Zhang, C., Wang, X., Jiang, C., et al. Numerical simulation of hot dry rock under the interplay between the heterogeneous fracture and stimulated reservoir volume. Journal of Cleaner Production, 2023, 414: 137724.

Zhao, N., You, F. Can renewable generation, energy storage and energy efficient technologies enable carbon neutral energy transition? Applied Energy, 2020, 279: 115889.

Zhou, X., Gao, Q., Chen, X., et al. Developmental status and challenges of GWHP and ATES in China. Renewable and Sustainable Energy Reviews, 2015, 42: 973-985.